Article

The assessment of the transversal rupture strength (TRS) and hardness of WC-Co specimens made via Additive Manufacturing and Sinter-HIP

Ovidiu-Darius Jucan [1,] *, Rareş-Vasile Gădălean[2,3] , Horea-Florin Chicinaş [1,2], Nicolae Bâlc [3] and Cătălin-Ovidiu Popa [1]

[1] Materials Science and Engineering Department, Technical University of Cluj-Napoca, 103-105, Muncii Avenue, 400641, Cluj-Napoca, Romania; dariusjucan@stm.utcluj.ro, catalin.popa@stm.utcluj.ro

[2] Gühring Romania, Constructorilor Street 32, 407035, Apahida, Romania horea.chicinas@stm.utcluj.ro

[3] Department of Manufacturing Engineering, Technical University of Cluj-Napoca, 103-105, Muncii Avenue, 400641 Cluj-Napoca, Romania; Nicolae.Balc@tcm.utcluj.ro; gadalean.rares.vasile@gmail.com

* Correspondence: dariusjucan@stm.utcluj.ro

Abstract: This study is focused on the mechanical properties of WC-Co composites obtained via Selective Laser Sintering using PA12 as a binder. The as-printed samples were thermally debonded, and sintered, first in vacuum, and then sinter-HIPed at 1400°C, using 50 bar Ar, which has led to relative densities up to 66 %. Optical metallographic images show a microstructure consisting of WC, with an average grain size in the range of 1.4 – 2.0 μm, with isolated large grains, in a well-distributed Co matrix. The shrinkage of the samples was 43 %, with no significant shape distortion. The printing direction of the samples has a great impact on the transversal rupture strength (TRS). Nevertheless, the bending strength was low, with a measured maximum of 612 MPa. SEM images of the fracture surface of TRS samples show the presence of defects that constitute the cause of the low measured values. The hardness values position the obtained composites in the range of medium coarse classical cemented carbides. The results were also related to the amount of free Co after sintering, close to the initial one, as assessed by magnetic measurements, indicating a low degree of interaction with PA12 decomposition products.

Keywords: WC-Co composite; Additive Manufacturing; Transversal Rupture Strength

1. Introduction

The WC-Co composites, known also as cemented carbides, are a class of materials well-known for their good combination between high hardness and toughness. Parts made of WC-Co are generally used in industries like mining, machining, cold forming, etc., where the wear properties play a significant role [1, 2]. The mechanical properties of cemented carbides are mostly influenced by the mean grain size of WC which is in the size range of 0.3 – 7.0 μm and the amount of Co, ranging from 3.0 to 30.0 % [3]. There are several pioneering studies concerning the mechanical properties of WC-Co, which theoretically and empirically explain the factors that influence the mechanical behavior of cemented carbides. A relationship between the hardness of WC-Co and the mean distance between carbide grains was found to be viable, which can be related to its microstructure [4]. In ultra-fine cemented carbide grade, where WC grain size is < 0.5 μm, the parts exhibit high hardness, thus high wear resistance, due to the prevention of abrasive materials to penetrate in depth.

The manufacturing route of cemented carbides is carried out by Powder Metallurgy methods, where the raw materials are first homogenized, then pressed depending on the geometrical complexity, followed by green machining and liquid phase sintering. Often, the green body is pre-sintered to increase the necessary strength to withstand the machining operation, which has the purpose of imposing the geometrical features. The traditional manufacturing process of cemented carbide parts involves high costs generated by the machining of green or pre-sintered parts in the

 doi:10.20944/preprints202305.0244.v1

case of high geometrical complexity parts and also by using dies which are intricate and costly to produce.

Additive manufacturing (AM) promises to overcome the limitations imposed by traditional manufacturing by eliminating the need for tooling and other manufacturing operations, overall reducing the manufacturing costs.

Up to this day, a few studies have been reported concerning AM of cemented carbides. Selective Laser Melting (SLM) sits at the top of the list of AM techniques used in WC-Co processing. Anyway, in the case of cemented carbides, the processes that develop high temperatures during the layer by layer processing lead to decarburization, chemical imbalances and Co evaporation [5]. During the repeated heating-cooling cycles of layer by layer building up, the Co behavior is different to the case of the traditional sintering process. Moreover, WC decomposes when exposed to high temperatures [6].

Binder Jetting (BJ) is a relatively new AM process, which involves the employment of a binder to selectively glue areas from the powder bed, thus the outcome of the printing process is a green body that requires further processing to increase the density. By using BJ, K. Enneti [7] successfully reached a near to the theoretical one density for a WC-12Co powder, using a 6.25 g/cm^3 apparent density raw - powder and sintering at 1485°C / 13 bars Ar pressure. The mechanical properties and microstructural results were similar to theWC-12Co medium grain size parts produced by the traditional manufacturing route. Furthermore, it has been proven that WC-Co produced by BJ has appropriate mechanical properties which confer to BJ a high potential in the manufacturing of WC-Co [8].

In contrast to BJ and SLM, Indirect Selective Laser Sintering (SLS) uses a low power laser to selectively melt areas from the powder bed, consequently creating necks between the particles. In SLS of WC-Co, a mixture of cemented carbide powder and a polymer binder is first printed layer by layer using a standard 3D printer. The printed object is then subjected to a heat treatment process that removes the polymer binder, leaving behind a "green" cemented carbide part that is still porous and fragile. This green part is then sintered in a high-temperature furnace to create a final dense and strong cemented carbide part. The main advantage using SLS in printing cemented carbide parts is that no support structures are needed, due to the surrounding powder from the powder bed which act as support structure for the printed parts. Secondly, it allows freedom of design since the parts are produced in a layer-by-layer fashion, where complex structures can be printed, with intricated cooling channels. The process usually takes place in N_2, at low temperatures, below the melting point or glass transition temperature of the organic binder. The SLS was employed in the processing of metallic and ceramic materials together with an organic binder [9-14]. The purpose of the organic binder is to melt under the laser beam to create bonds between the particles. In this way the parts resulted from the printing process are in green state. Therefore, the as printed parts undergo no deleterious operations specific with using high processing temperatures like in the case of SLM [5]. By using SLS in printing WC-Co parts, it allows the green parts to be processed in a similar manner with the parts that are conventionally produced. The as-printed green parts are thermally de-binded in order to remove the organic binder used in the printing process. Subsequent of the debinding operation liquid phase sintering (LPS) is talking place further densify the parts. During LPS, densification mechanisms like rearrangement, solution-reprecipitation and solid phase sintering are active to facilitate the densification of the part. Aside of our previous work [15], based on our knowledge, no other studies have been reported of WC-Co produced via SLS and sinter-HIP using an industrial approach, and its mechanical properties assessed. In this study, we are looking at the manufacturing of cemented carbide parts via SLS followed by Sinter-HIP and the assessment of their mechanical properties like hardness and mechanical strength.

2. Materials and Methods

The employed cemented carbide is a commercial ready to press spray-dried spherical particles WC-12Co powder (GTP, USA) with 34 μm median size, used as received. The powder exhibits good flowing while its bulk density is 2.90 g / cm^3, being a typical powder used in the traditional

Preprints (www.preprints.org) | NOT PEER-REVIEWED | Posted: 4 May 2023 doi:10.20944/preprints202305.0244.v1

manufacturing of cemented carbides. As an organic binder for the building of green specimens, commercial Polyamide PA12 powder (ALM, PA650, Germany) has been used as received. Polyamide, commonly known as nylon, is a popular material for additive manufacturing, due to its unique properties. Polyamide is a thermoplastic material that can be melted and re-solidified repeatedly without any significant changes to its properties, making it suitable for use in additive manufacturing processes like selective laser sintering (SLS). The PA12 powder shows a bulk density of 0.46 g / cm^3, while the average particle size is 55 μm, being a well-known material used in SLS. Details regarding the WC-Co and PA12 powders properties used can be found in our prior study [15]. The appropriate content of PA12 is 20 wt. %, found in our previous research to print stable green specimens. Figure 1 shows the morphology of the WC-12Co and PA12 powders used in this study. WC-12Co powder has spherical hollow granules with diameters in the range of 10 – 74 μm, with a relative porous microstructure; pores are relatively uniform distributed within granules walls, Figure 1a. PA12 binder particles display a spherical shape, and the average diameter is situated around 55 μm, Figure 1b. The mixture consisted of WC-12Co – 20 wt. % PA12, which has been homogenized for 4h using a 3D industrial mixer. Cube samples of 20 x 20 mm were printed together with samples of Φ4.6 x 35 mm used for the transversal rupture strength (TRS) test. A commercial machine, Sintering 2000 (DTM Corporation/3DSystems, USA) equipped with a 50 W CO_2 laser, was used for printing the green samples. The printing process was performed in N_2 atmosphere to avoid thermal oxidation while the parts were produced with the part bed temperature set to 170°C.

The as-printed green specimens are thermally de-binded at 800°C for 4 h to remove completely the organic binder, followed by sintering in vacuum at 1400°C for 2 h using a PVA Tepla / Pfeiffer Balzers COV 733 R industrial furnace. Subsequently, sintering in vacuum was performed at 1200°C followed by HIP at 1400°C with 50 bar Ar for 1 h, using an ALD VKP 50/50/170 industrial sinter-HIP furnace. The dimensions of the cube shape samples were measured after each sintering cycle to calculate the shrinkage. Density determination was performed by the gravimetric method.

Figure 1. Morphology of WC-12Co powder (a) and PA12 powder (b).

The free cobalt content of sintered samples was assessed by magnetic measurements using a Förster Koerzimat 1.097 HCJ unit. The sintered samples were polished and etched using Murakami reagent for metallographic analysis using a Leica DM6000 M optical microscope. For the green and sintered samples' microstructural characterization, a Sigma Zeiss scanning electron microscope (SEM) was used as well. The Vickers hardness test has been performed using a FISCHERSCOPE HM2000 equipment with a 0.3 kgf indentation force. The mechanical strength has been evaluated by using the 3-point bending test known also as transversal rupture strength, accordingly with DIN 3327 and ISO 3327, using a Zwick UPM 1475 with Zmart Pro machine test.

3. Results

A low powder bulk density can lead to voids, porosity, and weaker mechanical properties in the final part. A high powder bulk density can also lead to a more uniform energy absorption dur-

Preprints (www.preprints.org) | NOT PEER-REVIEWED | Posted: 4 May 2023 doi:10.20944/preprints202305.0244.v1

ing laser exposure, which can result in a more uniform melting and sintering process.The green samples processed by SLS showed low relative densities (around 15 %), due to the low bulk density of the starting powder and to the high amount of PA12 (20 %) which decreases density overall. Selective laser sintering is categorized as a powder bed process, the parts are 3D printed whereas no pressure is applied in order to increase the contact between particles. Therefore, the green density of the printed parts is almost equivalent with the bulk density of the powder mixture that is used. Due to low green density and high organic binder content (20 %) the samples have undergone shrinkage up to 43 % during debinding, vacuum sintering and the sinter-HIP process, exceeding the shrinkage that takes place in processes like MIM (metal injection moulding) [16] or even Binder Jetting [7]. In Figure 2 is presented the contrast between cube shape samples before and after the debinding and sintering process. There is a big difference between samples before and after sintering, showing the high shrinkage that has occurred during the process. Concerning the sintered sample, the uneven deformation that has taken place due to the friction with the support during sintering can be noticed, a phenomenon also known as “elephant foot”. The term "elephant foot" is used to describe a condition where the bottom surface of a sintered part has a bulging or flattened appearance. In green state, the samples contained three phases: WC-Co granules, previously molten PA12 and pores, while after sintering, the organic binder removal led to new pores formation. The densification that occurred during the debinding and liquid phase sintering process of was significant with respect to the green density, indicating the removal of a high proportion of the pores, though not enough to attain appropriate densification that is normally needed in metal cutting industry.

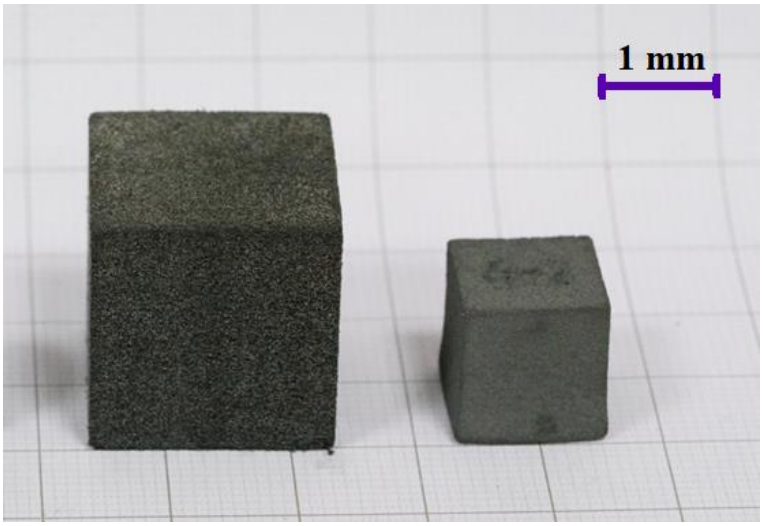

Figure 2. Contrast between cube shape samples before and after the debinding- sintering process, showing the shrinkage.

Samples have presented low relative densities after vacuum sintering and sinter-HIP, the WC-12Co, Table 1. The relative ineffectiveness of sinter-HIP is related to the open porosity present within the samples, which hinders the pore closure. In order to have an effective densification during sinter-HIP, close porosity is needed, therefore at higher levels of densification. The low densification after the sintering process is due to the low green density generated by the high amount of PA12 and to the low bulk density of the starting powder. In Figure 3 is presented the microstructure after sintering of the WC-12Co specimens.

Preprints (www.preprints.org) | NOT PEER-REVIEWED | Posted: 4 May 2023 doi:10.20944/preprints202305.0244.v1

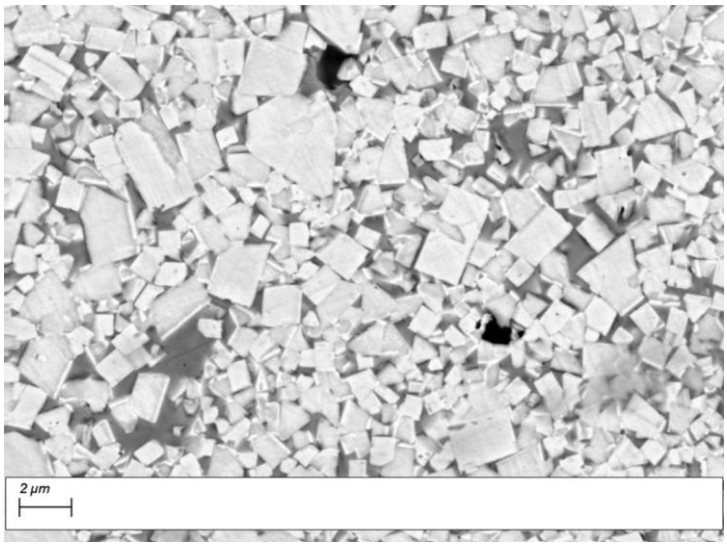

Figure 3. SEM image with the microstructure of sintered WC-12Co + 20 % PA12.

The microstructure is similar to the medium grain size cemented carbide grade, consisting of 1.4 – 2.0 µm grain in a well-distributed Co matrix. As sustained by the data in literature, generally, sintering in inert gases acts as an inhibitor of excessive grain increasing, facilitating microstructure refinement [17, 18]. There also can be found small and large pores which have not been removed during the sintering process and also rich cobalt areas which are considered to be former pores that have been filled with liquid phase during sintering.

The properties of the WC-Co specimens are presented in Table 1. The magnetic measurements show a high magnetization generated by high organic residues after PA12 decomposition. The free cobalt content in cemented carbides refers to the amount of cobalt that is not bound to the carbide phase and is present as metallic cobalt in the material. At the same time, the free ferromagnetic Co is 10.8 %, which leads to the conclusion that a small amount of the metal binder has reacted and formed compounds during sintering, due to the high amount of carbon. More details about the magnetic measurements and structural characterization can be found in our previous work [15].

Table 1. Properties of the WC-Co samples.

ρ_{green} [%]	$\rho_{vacuum\text{-}sintered}$ [%]	$\rho_{sinter\text{-}HIP}$ [%]	M_s [gsscm³/g]	H_c[Oe]	Shrinkage[%]	% free Co
15	61.3	66	217	148	43	10.8

Transverse rupture strength also known as bending strength test, represents the most common way to assess the mechanical strength of cemented carbides. The specimens of a specified length, with a chamfered, rectangular cross-section are placed on two supports and loaded centrally until the fracture occurs accordingly to the standardized DIN 3327 3-bending test method. The mechanical strength of cemented carbides depends on several factors, including the type and amount of carbide phase, the size and distribution of the carbide particles, and the quality of the metal binder. The test involves placing a sample of the material across two supports and applying a load at the center of the sample using a third support. The load is gradually increased until the sample breaks. The TRS is then calculated by dividing the maximum load applied by the cross-sectional area of the sample. The specimens were sintered and ground before undergoing the test. In Figure 4 are presented the plotted TRS values for the WC-Co samples in comparison with the TRS values of cemented carbides conventionally manufactured by the Powder Metallurgy route [19]. It has been noticed that for the WC-12Co samples built vertically during the printing process, higher mechanical strength (612 MPa) has been obtained compared with the samples horizontally built (328 MPa). The difference between TRS values of the samples is related to the printing direction of the green samples during the SLS process, since the obtained structure is not isotropic. Cemented carbides, typically exhibit anisotropic mechanical properties due to the directional nature of the carbide par-

Preprints (www.preprints.org) | NOT PEER-REVIEWED | Posted: 4 May 2023 doi:10.20944/preprints202305.0244.v1

ticles. The orientation of the carbide particles and their distribution in the metallic binder can affect the mechanical properties of the material in different directions. Regardless of the TRS values obtained for the WC-12Co processed by SLS and sinter-HIP, the transversal rupture strength is too low compared with the TRS of cemented carbides conventionally processed by Powder Metallurgy for the same WC-Co powder grade, this being highly related to the final density of the parts. According to Figure 4, the same cemented carbide grade, manufactured in the conventional way, shows a mechanical strength four times higher (2840 MPa) than the WC-Co processed in this study.

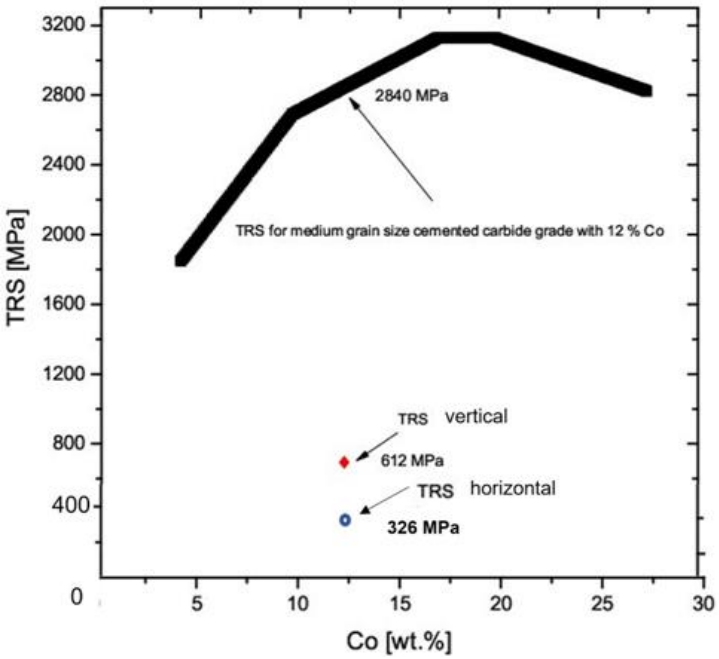

Figure 4. Mechanical strength of WC-12Co compared with the data in literature regarding typical cemented carbides produced by the traditional manufacturing route (PM), [19, 20].

The Vickers hardness test led to an average of 1285 HV30 as a result of four measurements. In Figure 5 are shown the results of the hardness test together with the indentation marks made on the microstructure of the WC-Co specimens. Even though the average hardness values obtained on the samples processed by the SLS are similar to the values obtained on samples processed by BJ [7] for the medium grain size cemented carbide grade, there is a big difference between the four hardness measurements that have been performed. We consider that the reason behind the wide hardness values range is the porosity within the specimens, although the measured areas do not present visible porosity on the surface where the indentation has been performed.

Preprints (www.preprints.org) | NOT PEER-REVIEWED | Posted: 4 May 2023 doi:10.20944/preprints202305.0244.v1

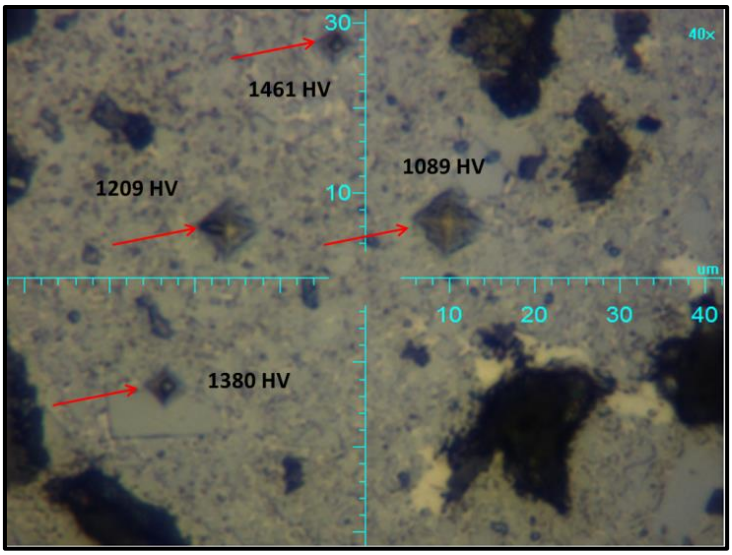

Figure 5. Vickers hardness test performed with 0.3 kgf on the WC-12Co specimens processed via SLS and Sinter-HIP.

In figure 6 is presented the evolution of hardness as a function of cobalt content for cemented carbide grades manufacured by the traditional way [19]. The hardness measured on the WC-12Co specimens processed by SLS and sinter-HIP fits in the hardness range at the border of the cemented carbides with medium grain size (1.2 – 2.0 μm) and medium coarse size (2.1 – 3.4 μm) with 12 % Co, Figure 6, it is comparable with the hardness of the typical cemented carbides grades as a function of the cobalt content for cemented carbides manufactured by the conventional way with the same WC grain size [17]. This shows that the SLS followed by Sinter-HIP has the potential to obtain cemented carbide parts that are usable for certain applications, where the need for a given hardness (wear resistance) prevails over the need for high strength.

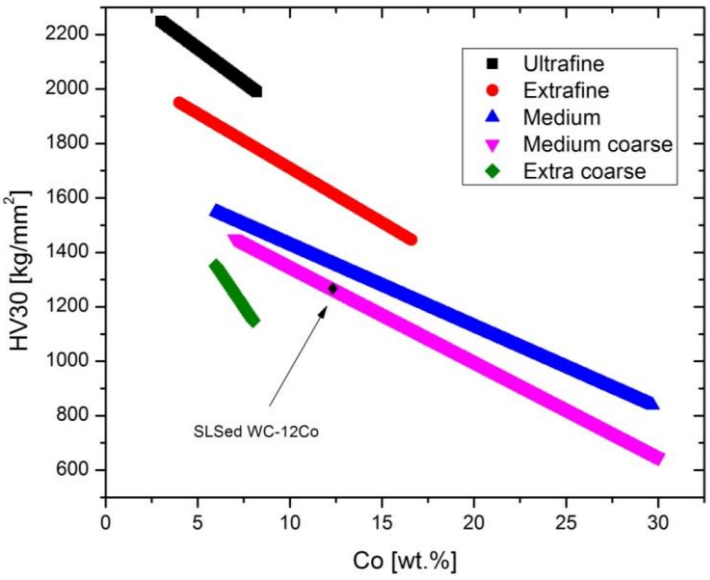

Figure 6. Vickers hardness of WC-12C of samples processed by SLS and Sinter-HIP versus the typical hardness of different grades of cemented carbides produced by Powder Metallurgy [19, 20].

In SLS, the printing direction can have a significant influence on the quality of the final product. When printing in different directions, the orientation of the object can affect the strength, surface finish, and overall quality of the final product. The printing direction can also affect the strength and mechanical properties of the final product. The fracture surface resulted after the bending test, was examined by SEM for the broken TRS specimens built horizontally and vertically,

Preprints (www.preprints.org) | NOT PEER-REVIEWED | Posted: 4 May 2023 doi:10.20944/preprints202305.0244.v1

Figure 7. Regardless of the magnification, the porosity can be seen throughout the entire surface of the fractured samples, fact in good agreement with the data in literature [21, 22]. Porosity can have a significant impact on the properties of cemented carbides. It can reduce the strength, toughness, and wear resistance of the material. Porosity can also act as stress concentrators, leading to premature failure of the material under load. The source of the high porosity is the high amount of organic binder used in the SLS process (20 wt. %) and the residual voids left after the printing process due to hollow WC-Co particles. It can be noticed that for the TRS samples built horizontally, Figures 7b and c, the shape of the former granules of the agglomerates have been flattened, while the samples built vertically have maintained their shape, Figures 7e and f.

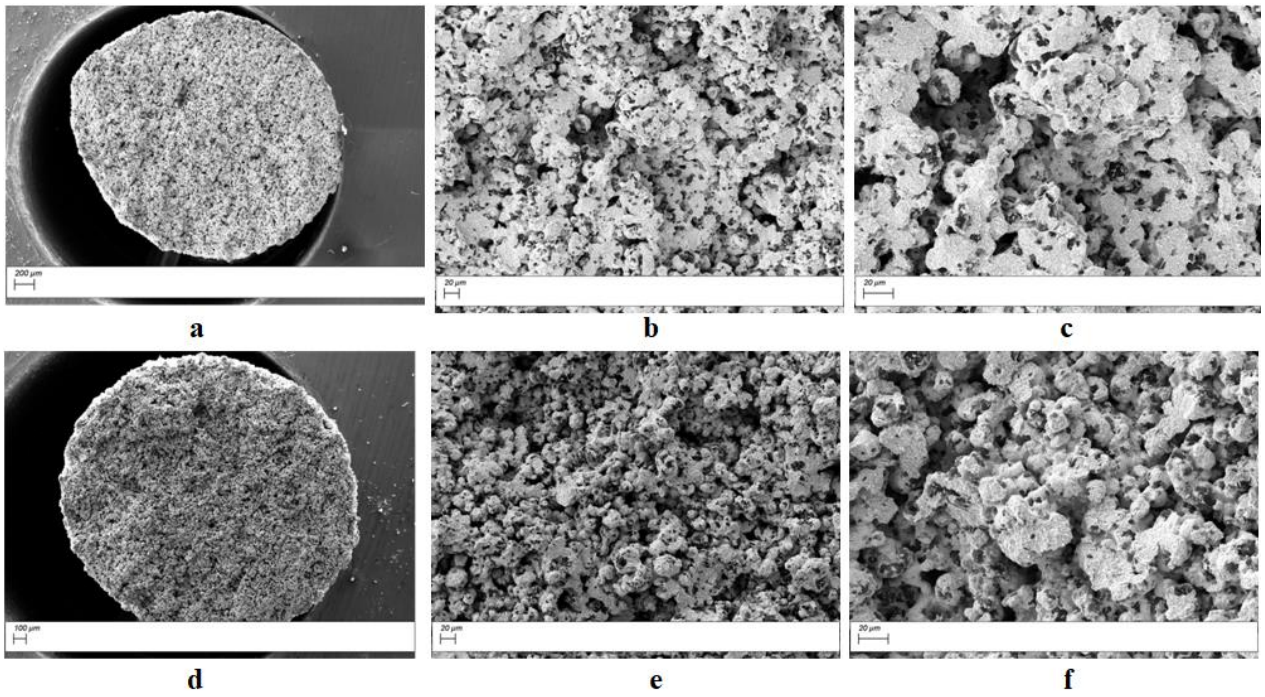

Figure 7. SEM images of the TRS fracture surface of WC-12Co samples built horizontally: a) low magnification, b) average magnification and c) high magnification; and WC-12Co samples built vertically: d) low magnification, e) average magnification and f) high magnification.

A horizontal approach used in the printing of the TRS samples has provided a much higher packing density of the particles, easing the diffusion processes and other densification mechanisms to be active, while for the samples built vertically, the formation of the liquid phase and rearrangement of particles constituted the main mechanisms by which the sintering necks have been created.

The failure of WC-12Co cemented carbides is a matter of the sintered particles resistance under various solicitations in working conditions. The behaviour of such materials was modelled and investigated by the machine learning algorithms based on a neural network approach. It was found that the wear resistance is improved by the reduction of the grain size and the high temperature crack resistance might be improved by addition of some rare earth such as La [23, 24].

4. Conclusions

This study was carried out to assess the mechanical properties of indirect SLS 3D printed (SLS) WC-Co / PA12 composites. The sintered samples displayed relative densities up to 66 %, while the shrinkage of the cube - shape samples has been up to 43 %. The microstructure contained WC grains within the 1.4 – 2.0 μm size range, with only isolated large WC grains. The TRS test has shown a low mechanical strength, up to 612 MPa for the samples vertically built, while for the samples built horizontally, the mechanical strength is even lower, due to the residual porosity after sinter-HIP. The Vickers hardness test led to an average hardness of 1285 HV30 being situated at the border of cemented carbide medium and medium coarse grades traditionally manufactured. The

SEM image of the fracture surfaces of the TRS samples has shown the high residual porosity that can be found throughout the entire volume. The obtained results show, on one hand, the limitations of the process involving SLS for the manufacturing of WC-12Co parts and, on the other, the potential to develop the method for producing of certain cemented carbide parts, with complex shapes, in small production scales.

Author Contributions: Conceptualization, O.D.J. and C.O.P.; methodology, O.D.J and H.C.; software, O.D.J; validation, C.O.P, H.C. and N.B.; formal analysis, R.V.G.; investigation, R.V.G.; resources, O.D.J.; data curation, C.O.P.; writing—original draft preparation, O.D.J.; writing—review and editing, O.D.J and C.O.P.; visualization, N.B.; supervision, C.O.P and H.C.; project administration, H.C.; funding acquisition, H.C and R.V.G. All authors have read and agreed to the published version of the manuscript.

Funding: This research was financially supported by the Project "Entrepreneurial competences and excellence research in doctoral and postdoctoral programs - ANTREDOC", project co-funded by the European Social Fund financing agreement no. 56437/24.07.2019.585 This work was supported by the european development Fund and theRomanian Government through the competitiveness Operational Pro-gramme 2014-2020, project id P 34 466, MySMiS code 121349, contract no.5/05.06.2018. The generous support of the Gühring company in making this work possible is highly acknowledged. This work was made possible by the generous support of the Gühring Company.

Data Availability Statement: Data are available on request from the correspondent author.

Acknowledgments: In this section, you can acknowledge any support given which is not covered by the author contribution or funding sections. This may include administrative and technical support, or donations in kind (e.g., materials used for experiments).

Conflicts of Interest: The authors declare no conflict of interest.

References

1. Bricín, D.; Ackermann, M.; Jansa, Z.; Kubátová, D.; Kříž, A.; Špirit, Z.; Šafka, J. Development of the Structure of Cemented Carbides during Their Processing by SLM and HIP. *Metals* **2020**, *10*, 1477. https://doi.org/10.3390/met10111477
2. Fang, S.; Salán, N.; Pauly, C.; Llanes, L.; Mücklich, F. Critical Assessment of Two-Dimensional Methods for the Microstructural Characterization of Cemented Carbides. Metals **2022**, 12, 1882. https://doi.org/10.3390/met12111882
3. Sarin, V. K. Comprehensive Hard Materials, in *Hardmetals*, Daniele Mari and Luis Llanes, Eds., **2014**, 1–100.
4. Lee, H. C.; Gurland, J. Hardness and deformation of cemented tungsten carbide,*Materials Science and Engineering*, **1978**, 33, 125–133, doi: 10.1016/0025-5416(78)90163-5.
5. Uhlmann, E.; Bergmann, A.; Gridin, W. Investigation on Additive Manufacturing of Tungsten Carbide-cobalt by Selective Laser Melting, *Procedia CIRP*, **2015**, 35, 8–15, doi: 10.1016/j.procir.2015.08.060.
6. Kurlov, A. S.; Gusev, A.I. Tungsten Carbides and W – C Phase Diagram, **2006**, 42, 121–127, doi: 10.1134/S0020168506020051.
7. Enneti, R. K.; Prough, K. C.; Wolfe, T. A.; Klein, A.; Studley, N.; Trasorras, J. L. Sintering of WC-12%Co processed by binder jet 3D printing (BJ3DP) technology, *Int J Refract Metals Hard Mater*, **2017**, 71,28–35, doi: 10.1016/j.ijrmhm.2017.10.023.
8. Enneti, R. K.; Prough, K. C. Wear properties of sintered WC-12%Co processed via Binder Jet 3D Printing (BJ3DP)," *Int J Refract Metals Hard Mater*, **2018**, 78, 228-232, doi: 10.1016/j.ijrmhm.2018.10.003.
9. Deckers, J.; Shahzad, K.; Vleugels, J.; Kruth, J.P. Isostatic pressing assisted indirect selective laser sintering of alumina components,*Rapid Prototyp J*, **2012**, 18, 409–419, doi: 10.1108/13552541211250409.
10. Liu, K.; Shi, Y.; He, W.; Li, C.; Wei, Q.; Liu, J. Densification of alumina components via indirect selective laser sintering combined with isostatic pressing, *International Journal of Advanced Manufacturing Technology*, **2013**, 67, 2511–2519, doi: 10.1007/s00170-012-4668-0.

11. Liu K. *et al.*, Research on selective laser sintering of Kaolin-epoxy resin ceramic powders combined with cold isostatic pressing and sintering, *Ceram Int*, **2016**, 42, 10711–10718, doi: 10.1016/j.ceramint.2016.03.190.
12. Yan, C. Z.; Shi, Y. S.; Yang, J. S.; Liu, J. H. Preparation and selective laser sintering of nylon-coated metal powders for the indirect SLS process,**2008**, 5, 355–360, doi: 10.1108/13552540910993888.
13. Shahzad, K.; Deckers, J.; Zhang, Z.; Kruth, J. P.; Vleugels, J. Additive manufacturing of zirconia parts by indirect selective laser sintering, *J Eur Ceram Soc*, **2014**, 34, 81–89, doi: 10.1016/j.jeurceramsoc.2013.07.023.
14. Shahzad, K.; Deckers, J.; Kruth, J. P.; Vleugels, J. Additive manufacturing of alumina parts by indirect selective laser sintering and post processing, *J Mater Process Technol*, **2013**, 213, 1484–1494, doi: 10.1016/j.jmatprotec.2013.03.014.
15. Jucan, O. D.; Gădălean, R. V.; Chicinaş, H. F.; Hering, M.; Bâlc, N.; Popa, C. O. Study on the indirect selective laser sintering (SLS) of WC-Co/PA12 powders for the manufacturing of cemented carbide parts, *Int J Refract Metals Hard Mater*, **2020**, 96, 105498, doi: 10.1016/j.ijrmhm.2021.105498.
16. Heng, S. Y.; Muhamad, N.; Sulong, A. B.; Fayyaz, A.; Amin, S. Y. M. Effect of sintering temperature on the mechanical and physical properties of WC–10%Co through micro-powder injection molding (μPIM), *Ceram Int*, **2013**, 39, 4457–4464, doi: https://doi.org/10.1016/j.ceramint.2012.11.039.
17. Xiang, Z.; Li, Z.; Chang, F.; Dai, P. Effect of Heat Treatment on the Microstructure and Properties of Ultrafine WC–Co Cemented Carbide. *Metals* **2019**, *9*, 1302. https://doi.org/10.3390/met9121302
18. Aleksandrov Fabijanić, T.; Jakovljević, S.; Franz, M.; Jeren, I. Influence of Grain Growth Inhibitors and Powder Size on the Properties of Ultrafine and Nanostructured Cemented Carbides Sintered in Hydrogen. Metals **2016**, 6, 198. https://doi.org/10.3390/met6090198
19. Understanding Cemented Carbides,Sandvik, Stockholm, Sweden.www.sandvik.com (Accessed November 2022)
20. Straumal, B.; Konyashin, I. WC-Based Cemented Carbides with High Entropy Alloyed Binders: A Review. *Metals* **2023**, *13*, 171. https://doi.org/10.3390/met13010171
21. Naughton-Duszová, A.; Csanádi, T.; Sedlák, R.; Hvizdoš, P.; Dusza, J. Small-Scale Mechanical Testing of Cemented Carbides from the Micro- to the Nano-Level: A Review. *Metals* **2019**, *9*, 502. https://doi.org/10.3390/met9050502
22. Chen, C.; Huang, B.; Liu, Z.; Li, Y.; Zou, D.; Liu, T.; Chang, Y.; Chen, L. Additive manufacturing of WC-Co cemented carbides: Process, microstructure, and mechanical properties, *Additive Manufacturing*, **2023**, 63, 103410, https://doi.org/10.1016/j.addma.2023.103410.
23. Guan, Z.; Tian, H.; Li, N.; Long, J.; Zhang, W.; Du, Y. High-accuracy reliability evaluation for the WC–Co-based cemented carbides assisted by machine learning, *Ceramics International*, **2023**, 49, 613-624, https://doi.org/10.1016/j.ceramint.2022.09.030.
24. He, M.; Zheng, X.; Tian, H.; Mao, H.; Du, Y. Residual thermal stress, fracture toughness, and hardness in WC-Co cemented carbide: Finite element simulation and experimental verification, *Journal of Materials Research and Technology*,**2022**, 21, 2445-2454, https://doi.org/10.1016/j.jmrt.2022.10.065.